The Protein Environment Drives Selectivity for Sulfide Oxidation by an Artificial Metalloenzyme

ARTICLE *in* CHEMBIOCHEM · FEBRUARY 2009

Impact Factor: 3.09 · DOI: 10.1002/cbic.200800595 · Source: PubMed

8 AUTHORS, INCLUDING:

Pierre Rousselot-Pailley
French National Centre for Scientific Resea…
23 PUBLICATIONS **422** CITATIONS
SEE PROFILE

Constance Bochot
University Joseph Fourier - Grenoble 1
13 PUBLICATIONS **122** CITATIONS
SEE PROFILE

Christine Cavazza
Atomic Energy and Alternative Energies Co…
48 PUBLICATIONS **2,311** CITATIONS
SEE PROFILE

Stéphane Ménage
Atomic Energy and Alternative Energies Co…
83 PUBLICATIONS **2,119** CITATIONS
SEE PROFILE

DOI: 10.1002/cbic.200800595

The Protein Environment Drives Selectivity for Sulfide Oxidation by an Artificial Metalloenzyme

Pierre Rousselot-Pailley,[a] Constance Bochot,[b] Caroline Marchi-Delapierre,[a] Adeline Jorge-Robin,[a] Lydie Martin,[b] Juan C. Fontecilla-Camps,[b] Christine Cavazza,*[b] and Stéphane Ménage*[a]

Artificial metalloenzymes based on the incorporation of Mn–salen complexes into human serum albumin display high efficiency and selectivity for sulfoxide production during sulfide oxidation. The reactions carried out by the artificial metallozymes are comparable to those carried out by natural biocatalysis. We have found that the polarity of the protein environment is crucial for selectivity and that a synergy between both partners of the hybrid results in the novel activity.

Introduction

Pressure from society has placed restrictions on industrial oxidation technology; this has emphasized the need for sustainable and environmentally friendly processes. Different strategies have generated both biological[1] and bioinspired catalytic approaches in an effort to fulfill the demands of "green chemistry." [2] Artificial metalloenzymes combine these two domains. These hybrids, created by the insertion of unnatural, active, metal sites into proteins, combine the specific properties of proteins and enzymes (substrate specificity and/or stereoselectivity) with those of nonbiological catalysts.[3–11] The main interest of these novel systems resides in the potential to apply man-made catalysts under biological catalytic conditions. Thus, the polypeptide chain transfers properties such as water solubility, solvent accessibility and a chiral environment to the inorganic catalyst. Moreover, the optimization of these catalysts is facilitated by the chemical modification of the catalyst ligands and by site-directed mutagenesis of the protein.

One of the main technological barriers for the synthesis of these hybrid molecules is the selective insertion of the active site into the protein. Several strategies have been used. Amino acid residues can be functionalized by organometallic moieties, as shown by the pioneering work of Kaiser et al.[12] Noncovalent interactions are also useful. Whitesides et al. pioneered the supramolecular approach known as the "Trojan horse." [13] It involves the modification of an enzyme substrate by a moiety containing the synthetic active site, and it is still the most successful approach. For example, the biotin-(strept)avidin system, in which biotin is modified in order to insert rhodium complexes, can afford very efficient enantioselective hydrogenation reactions.[14–17] Other noncovalent approaches for embedding catalysts in protein scaffolds have been recently validated. The introduction of metal-salen complexes into myoglobin is effective thanks to the coordination of the metal ion of the catalyst by a histidine residue.[18] The binding of a porphyrin ring into serum albumin was made possible by the introduction of sulfonated substituents.[19]

Examples of catalysis by these artificial metalloenzymes range from hydrolysis,[20] hydroxylation,[21] Diels–Alder reactions[22a] and hydroformylation[22b] to hydrogenase activity.[14–17] However, examples of selective oxygenases are rather scarce.[23–27] Enantioselective sulfide oxidations have been recently obtained with an enantiomeric excess (*ee*) of up to 70% with iron or Mn corroles bound to human serum albumin (HSA).[28]

The optimization of these bioinorganic catalysts is then of great interest, and requires the elucidation of the principles governing the activity of artificial metalloenzymes. Among these principles, the contribution of the protein scaffold to the selectivity and stability needs to be assessed. A suitable hybrid should have a genuine original property when compared to its two separate components. This could be accomplished, for instance, by the tuning of the selectivity by the hydrophobicity of the inorganic catalyst binding site in a protein. Herein, we report the design of novel Mn monooxygenase mimics obtained by the insertion of Mn^{III}-salen complexes into HSA. Such hybrids are very efficient, stable and selective biocatalysts and are easy to handle in aqueous medium for the sulfide oxidation by sodium hypochlorite. The impact of the protein environment on both reactivity and selectivity is discussed, and

[a] *Dr. P. Rousselot-Pailley, Dr. C. Marchi-Delapierre, A. Jorge-Robin, Dr. S. Ménage*
Laboratoire de Chimie et Biologie des Métaux, Université Joseph Fourier
UMR 5249-CNRS, IRTSVCEA–Grenoble
17 avenue des Martyrs, 38054 Grenoble Cedex (France)
Fax: (+33) 4-38-78-91-06
E-mail: smenage@cea.fr

[b] *Dr. C. Bochot, L. Martin, Dr. J. C. Fontecilla-Camps, Dr. C. Cavazza*
Laboratoire de Cristallographie et de Cristallogénèse des Protéines
Institut de Biologie Structurale J.P. Ebel (CEA-CNRS-UJF)
41 rue Horowitz 38027 Grenoble Cedex 1 (France)
Fax: (+33) 4-38-78-51-22
E-mail: christine.cavazza@ibs.fr

Supporting information for this article is available on the WWW under http://www.chembiochem.org or from the author.

the properties of the hybrids are compared to those of the synthetic complex alone. We demonstrate that the protein environment induces the selective oxidation of sulfide to sulfoxide, in contrast to the inorganic catalyst, with which only sulfone is obtained. This work validates the artificial enzyme strategy for catalysis because activity values, in terms of both number of catalytic cycles and selectivity, are close to those of enzymes.

Results and Discussion

The design of artificial enzymes requires the selection of a protein capable of binding a catalyst that will drive the targeted reaction. In this context of supramolecular anchoring of cofactors, serum albumin plays a key role; it functions as a transport protein in plasma and shows a unique ability to bind a variety of hydrophobic molecules, including steroids, fatty acids and heme.[29] In addition, serum albumins, especially the bovine one, have been shown to catalyze enantioselective transformations such as oxidations,[30,31] reductions[32] and Diels–Alder cycloadditions with moderate to good enantioselectivity.[33] We have chosen Mn–salen catalysts, which are well-known systems for selective oxidation catalysis in organic solvents, because of their broad catalytic properties.[34] The hybrids were characterized in terms of complex location and sulfide oxidation catalytic properties.

Synthesis of new artificial metalloenzymes

The design of these artificial metalloenzymes was based on the embedding of Mn–salen complexes into HSA through supramolecular anchoring. Several Mn–salen derivatives were synthesized (Scheme 1) in order to optimize the stability of the

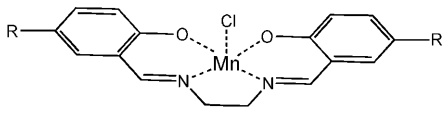

R = H complex 1
R= COOH 2
R = SO_3H 3
R = OH 4

Scheme 1. Mn–salen complexes used in this study.

resulting hybrid⊂HSA (the formalism **1**⊂HSA refers to the hybrid with complex **1**)[7] as a function of the polarity of the R substituents.[35] Three R groups, in addition to R = H, were chosen with pK_a values ranging from −1 to −9 for sulfonate, carboxylate and hydroxyl moieties, respectively.

The ligand synthesis was adapted from published procedures, based on the reaction of 2 equiv. of the R substituted salicylaldehyde with 1 equiv of ethylenediamine in methanol (see the Experimental Section). The complex was formed by the reaction of $Mn(OAc)_2{\cdot}4H_2O$ with 1 equiv. of the salen ligand in aerated ethanol in the presence of excess lithium chloride. Complexes **1**–**3** were soluble in water or buffered solution at pH 8.0. Complex **4** was barely soluble under these conditions.

Initially, the hybrids were prepared by incubating 1 equiv. of HSA with 10 equiv. of Mn complex overnight. The excess complex was subsequently removed. All the hybrids were colored, attesting to the presence of the Mn complex in the protein. The addition of protein to an aqueous suspension containing complex **4** led to its solubilization, suggesting that it formed a hybrid with HSA.

The Mn content in the hybrids was determined by inductively coupled plasma (ICP) and the protein concentration by quantitative amino acid analysis (the standard Bradford method[36] overestimated the protein concentration, probably due to interference by the metal complex). The Mn/protein ratio of the hybrids varied from 1 to 4, depending on the R substituents of the salen ligand (Scheme 1, Table 1); the unsubstituted Mn–salen complex **1** binds to multiple sites (up to four), whereas the substituted ones were bound more specifically.

Table 1. Physical properties of Mn–salen/HSA hybrids.

Complex	**1**	**2**	**3**	**4**
R substituent	H	CO_2H	SO_3H	OH
Mn/HSA ratio[a]	4 ± 0.5	1.6 ± 0.8	1 ± 0.2	2 ± 0.5
UV–visible[b] λ [nm]	–	395 (1600)	385 (1800)	465 (8000)
(ε [$M^{-1}cm^{-1}$])		280	280	325 (40000)
				280
K_d [μM]	–	8	11	>40

[a] Error based on three dosages. [b] pH 8; molar extinction coefficient based on Mn content.

A second synthetic procedure was carried out in order to minimize the multiple binding of the complexes. The hybrids, except **4**⊂HSA, were synthesized by incubating equimolar amounts of HSA and Mn–salen complex for one hour in a buffered solution (pH 7.5) at room temperature with no further purification.

Spectroscopic characterization of the hybrids

Because of its high Mn/HSA ratio, **1**⊂HSA was excluded from the following characterization studies. The spectroscopic features presented below are identical regardless of the hybrid synthesis procedure.

With the exception of complex **4**, the UV–visible spectra of the Mn–salen/HSA hybrids were dominated by a single charge transfer (CT) band in the visible region, in addition to the 280 nm band attributed to the absorption of the protein and the complex (Figure 1). The spectrum of **4**⊂HSA depicted an extra intense CT band at 325 nm (Table 1). On the other hand, the spectra of the complexes in the absence of HSA are dominated by at least three more or less resolved transitions under 400 nm. In all cases, the visible transitions of the hybrids were different from those of the free synthetic complexes, revealing the presence of interactions between the complex and the po-

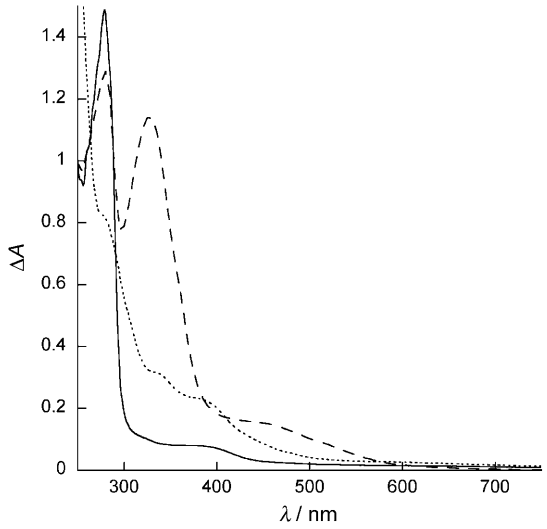

Figure 1. UV–visible spectra of complex **3** (····), hybrid **3**⊂HSA (—, 45 μM) and hybrid **4**⊂HSA (– – –, 23 μM) in buffered Tris solution (pH 8, 0.04 M).

lypeptide. When increasing amounts of complex **2** were added to an HSA solution at pH 7.5, the intensity of the 400 nm band augmented until a 1:1 mole ratio was reached. The further addition of complex **2** did not increase the intensity of this band. A new, less well-defined transition band around 360 nm, corresponding to unbound complex **2**, was then observed (data not shown).

The extinction coefficient and the energy of the transition bands depended on the nature of R. Also, the UV spectra were not as well-defined as those of Mn–salen complexes bound to an engineered myoglobin.[18,25,26] The differences between all these related systems could be due to the modification of the coordination sphere and/or possible electrostatic interactions between the deprotonated R substituent and different amino acid residues of the protein.

CD experiments were performed above 250 nm in order to both confirm the interactions between complexes **2** and **3** and the protein and assess the impact of the inorganic complex on the protein environment. Figure 2 shows that the presence of

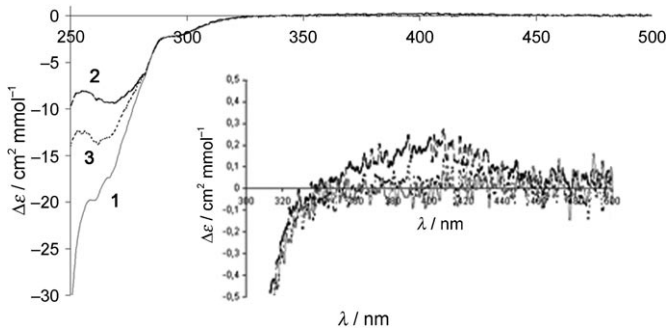

Figure 2. CD spectra of 30 μM of HSA (1), **2**⊂HSA (2) and **3**⊂HSA (3) at pH 7.5. Observed changes are related to the binding of the Mn–salen complex. A positive deviation in the visible region is related to the close interaction between the complex and the protein. Inset: expansion of the 300–450 nm region of the CD spectrum.

complex **2** or **3** affects the CD spectrum of the protein by reducing the negative signal at 275 nm and inducing a slight blue shift. These transitions can be correlated to α helices rearrangements due to complex binding to HSA. In addition, the CD spectra of **2**⊂HSA displayed a small positive deviation in the 400 nm region (Figure 2 inset). Since HSA, as opposed to the hybrid, does not absorb visible light, (Figure 1), this change can only be attributed to the interaction of complex **2** with the chiral environment of the protein.[19] This interaction was not observed in the case of complex **3** (Figure 2 inset).

The binding affinity of the Mn–salen complexes to HSA was studied by measuring the quenching of its UV fluorescence at pH 7.5. The emission of Trp214 ($\lambda_{max} = 340$ nm), as a function of complex **2** concentration, is shown in Figure S1 in the Supporting Information. The quenching was complete and selective, and suitable data were obtained from plots of fluorescence intensity versus HSA/complex ratio (Figure S1). K_d values were obtained from the initial monotonic decrease in fluorescence (Table 1). The fits indicated the presence of one high-affinity binding site per HSA molecule. Additional low-affinity sites were neglected in this study. The K_d values at pH 7.0 are in the μM range, with affinity increasing in the following order: complex **2** ≈ **3** > **4**.

The presence of ionizable R substituents improves the complex affinity. At pH 7.0, the R group was deprotonated in complexes **2** and **3** but not in complex **4**. This difference in polarity of the R group might explain the affinity trend. This also suggests that part of the bound complex environment is polar.

These complexes affinities are in the same range as those found for drugs known to be carried by HSA, such as thyroxine, ibuprofen and triiodobenzoic acid (TIB).[37,38]

Structural basis for binding of Mn–salen complexes

HSA has been extensively studied by X-ray crystallography and ^{1}H NMR, and binding sites for a wide range of drugs have been identified.[39] The protein binds a variety of endogenous ligands including the acidic non-esterified fatty acid, bilirubin, hemin, thyroxine and lipophilic compounds at many sites. HSA contains three homologous domains (I–III), each one comprising two sub-domains (A and B). To this date, six different binding sites have been structurally characterized: two primary sites called IIA and IIIA, and four other sites with lower binding affinities called IIIB, IIA-IIB, one site in domain IB and another in the cleft of the protein.[39]

The rather large number of binding sites in HSA makes it difficult to model the position of the complexes. So far, we have been unable to crystallize hybrids and, consequently, no X-ray structures are available. Consequently, we have carried out a series of competitive binding experiments between our complexes and targeted drugs in order to identify putative binding sites indirectly. The addition of these drugs to the hybrid solution could have two consequences. First, if a given drug and the inorganic complex share a binding site, the latter should be released to the solution, leading to the assignment of the site. Second, if the inorganic complex is not released, both molecules could simultaneously bind to the protein. This, in

turn, might induce structural changes resulting in a rearrangement of the two respective binding sites; that will be a function of the distance between them. For instance, a very recent study has shown that the addition of excess ibuprofen to heme-containing HSA influences the stability and the coordination mode of the heme.[40] The authors concluded that the binding sites were close, sharing one α helix.

CD spectroscopy is very sensitive to slight α helix movements; this makes it the spectroscopic tool of choice for our purpose. A spectral modification, other than the one arising from the simple superimposition of the respective drug⊂HSA and complex⊂HSA spectra, would indicate the proximity of the binding sites of both molecules. In order to determine the location of the inorganic complexes, several drugs with common HSA binding sites were used.

In the first experiment, four molecules, selected for their known HSA binding sites, were added separately to a **3**⊂HSA solution at a concentration above their K_d. Hemin for site IB, TIB for sites IB and IIA, thyroxine for sites IIA, IIIA, IIIB and the cleft and ibuprofen for sites IIA-IIB and IIIA. Their affinities ranged from nM in the case of hemin to μM for the others.[39] These molecules have both common and unique binding sites (Table 2). For example, thyroxine binds to five sites in HSA, two shared with ibuprofen or TIB. The latter also has a common site with hemin (Table 2).

Table 2. Binding sites in HSA for the molecules used in this study.

Binding site	Molecule
IB	hemin, TIB
IIA	thyroxine, TIB
IIA-IIB	ibuprofen
IIIA	thyroxine, ibuprofen
IIIB	thyroxine (two molecules)
cleft	thyroxine

After **3**⊂HSA or **2**⊂HSA were incubated overnight with each of these molecules at 277 K and pH 7.5, the solutions were dialyzed using a 5 kDa cut-off centricon® filter, and the filtrates were analyzed by UV/visible spectroscopy. Care was taken to use concentrations of hybrids and drugs above their respective K_d values. The number of binding sites was also taken into account in the calculation of the drug concentration to be used. Free complex **2** or **3** was only present in the filtrate from the thyroxine-containing solution. This experiment indicates that these complexes either bind to the cleft or to the IIIB site because they are specific for thyroxine. Moreover, the time for release was rather long (around 2 h) suggesting that the complex was bound to a low-affinity thyroxine site.

In order to discriminate between complex binding to the cleft or the IIIB site, we recorded the CD spectra of **2**⊂HSA and **3**⊂HSA and compared them to that of HSA in the presence of three different drugs. A superimposition of the resulting spectra is shown in Figure 3 for the **3**⊂HSA case. Thyroxine displayed a CD signal typical of a chiral molecule (black trace). The HSA spectrum (blue trace) is modified by the binding of

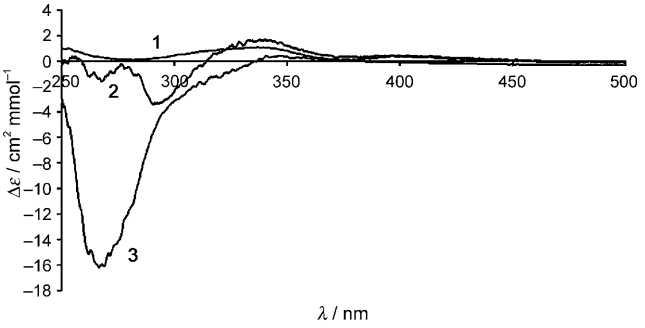

Figure 3. CD spectra of 250 μM thyroxine (1), 50 μM HSA plus 5 equiv. of thyroxine (2) and **3**⊂HSA plus 5 equiv. of thyroxine in Tris buffer, pH 7.5 (3). Observed changes are related to the binding of the drug even in the case of the hybrid. The location of the drug near the Mn–salen binding site is suggested.

thyroxine as shown by the presence of a negative CD signal centered at around 290 nm ($\Delta\varepsilon \approx -3$ cm^2 mmol^{-1}) and the loss of the 260 nm negative shift (see Figure 2). The corresponding signal was less well-defined when thyroxine was incubated with the **3**⊂HSA hybrid (red trace). In fact, a significant CD signal centered at 275 nm ($\Delta\varepsilon \approx -16$ cm^2 mmol^{-1}) dominated the spectrum.

In the case of **2**⊂HSA, a similar tendency was found for thyroxine as evidenced by a significant shoulder around 270 nm ($\Delta\varepsilon \approx -20$ cm^2 mmol^{-1}; Figure S2). The CD spectrum obtained with TIB as the competitive drug, showed a major change in the 300–250 nm region with the appearance of a positive transition under 265 nm for **3**⊂HSA (Figure S2). On the other hand, ibuprofen did not significantly affect the CD spectrum of either **2**⊂HSA or **3**⊂HSA.

The CD signal differences observed might have originated from a slight displacement of α helices (see above). Consequently, we examined the X-ray structure of HSA in search for an α helix between a TIB site and either the cleft or the IIIB site (Table 2).[39] Only the cleft site fulfills this requirement; this strongly suggests that it corresponds to the binding site for complexes **2** and **3**.

This conclusion was also supported by the quenching experiments, and indicates that the complex was bound close to Trp214. This residue is located at the bottom of the protein cleft, close to domain IIA (see Table 2). It has been recently demonstrated that the quenching by an acceptor located in subdomain IIIA will not take place because the probes are too far from the fluorophore.[41] Site IIIB can also be excluded on a similar basis.[39]

Based on the above experiments and the fluorescence study, we can propose that the Mn–salen **2** and **3** complexes bind to the cleft site of the protein.

Catalytic properties of Mn–salen⊂HSA hybrids

The oxidizing properties of the hybrids were assessed by comparing them with those reported for a few other systems.[25–28] The oxidation of thioanisole by NaOCl was monitored at room temperature under optimized conditions as follows: acetate

buffer (50 mM, pH 5.2), catalyst (125 μM) and a 1:200:100 ratio of catalyst/NaOCl/thioanisole. The catalyzed reactions were finished after 10 min. More basic pH values caused an increase in sulfone formation. The catalyst concentration was set at a higher value than the complex K_d in order to ensure the stoichiometry between the bound Mn complex and HSA. Control experiments were performed in reaction assays with protein and Mn^{II} salt, ligand alone and buffer. They all led to lower yields than those described in the following section.

The uncatalyzed reaction led to the exclusive formation of phenylmethylsulfone with a conversion yield of approximately 40%. When only HSA was present, both the yield and selectivity were altered, with a significant increase in selectivity for sulfoxide versus sulfone, combined with a 38 to 49% increase in the conversion. Catalysis was greatly improved with the hybrids (Table 3). The conversion was complete in most cases, except for **1**⊂HSA (75%), and the selectivity for sulfoxide was over 90%. Remarkably, with **2**⊂HSA, no trace of sulfone could be detected. The efficiency of **2**⊂HSA corresponded to 20 TON min^{-1} (turnover number min^{-1}. The opposite trend was observed for Mn–salen complexes in the absence of HSA; when complexes **1**–**4** were used as catalysts, only phenylmethylsulfone was detected with a conversion of approximately 60%. These results show that the hybrids have catalytic properties that are very different from those of either the free complexes or HSA alone.

Table 3. Catalytic properties of Mn–salen⊂HSA hybrids and Mn–salen complexes.

Catalyst	Conversion [%]	SO [%]/ SO_2 [%]	Selectivity for SO[a]
none	38	7/31	−63
HSA	49	39/10	59
1	62.5	0/62	−100
1⊂HSA	75	71/4	89
2	59	1/58	−96
2⊂HSA	97	97/0	100
2⊂HSA(5th)[b]	95	92/7	87
3	57	2/55	−92
3⊂HSA	81	80/1	99
3⊂HSA(5th)[b]	99	92/7	86
4	60	0/60	−100
4⊂HSA	91	86/5	90

[a] Selectivity = (%SO−%SO_2)/(%SO+%SO_2); SO = methylphenylsulfoxide; SO_2 = methylphenylsulfone; 100% corresponds to sulfoxides whereas −100% corresponds to sulfone. [b] After five successive additions of substrate and oxidant.

The existence of multiple sites in most of the hybrids, as shown by the Mn content, raises the question of their influence on the (enantio)selectivity of sulfide oxidation. To shed some light on this issue, we plotted the reaction yields versus the Mn–salen/HSA ratio at concentrations above the K_d. Figure 4 displays the evolution of sulfoxide yield and selectivity as a function of the number of equivalents of complex **2** or **3**. For both hybrids, the maximum yield and selectivity was observed at a Mn–salen/HSA ratio close to 1. This observation reinforces the conclusion that only one active site is responsible for the catalytic activity under normal conditions. This also agrees with the presence of a high-affinity binding site, as revealed by fluorescence quenching experiments. When the ratio exceeded 1, both the selectivity and yield decreased dramatically in each case. The increasing formation of sulfone as the Mn–salen content increases is then related to the activity of the free Mn–salen complex, indicating that the excess Mn–salen complex remains outside the protein under these conditions. Figure 4 also shows that the two hybrids displayed different reactivity patterns for Mn–salen/HSA ratios lower than 1. In the case of complex **2**, the selectivity, close to 100%, was only slightly affected by sub-stoichiometric concentrations of Mn–salen. On the other hand, in the case of complex **3**, the selectivity increased from 55 to 93% with increasing Mn–salen concentration. These observations correlate well with sulfoxide production; for example, for a Mn–salen/HSA ratio of 0.5, sulfoxide yields were 70% for complex **2** and 40% for complex **3**. Thus, **2**⊂HSA was more catalytically active than either **3**⊂HSA or HSA alone. In the case of complex **3**, the total observed activity corresponds to the sum of the formation of sulfone and sulfoxide, catalyzed by HSA and the hybrid, respectively. For complex **2**, sulfoxide production indicates that the hybrid activity overwhelms HSA-based catalysis.

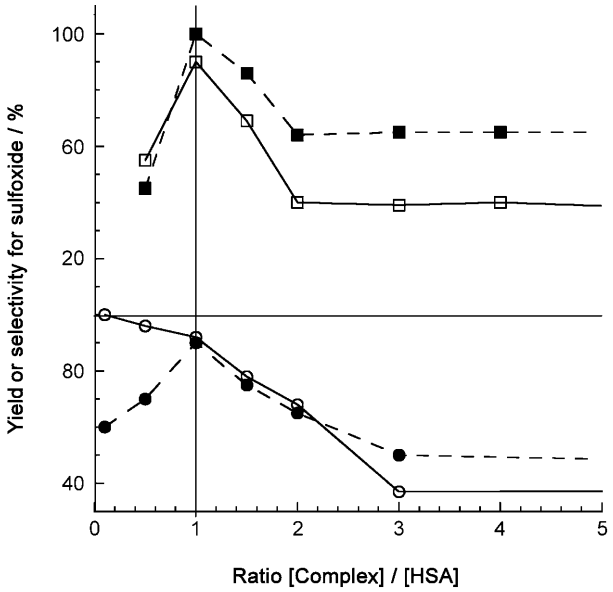

Figure 4. Yield (- - -) and selectivity (—) for sulfoxide formation as a function of the complex **2**/HSA (lower graph) and complex **3**/HSA (upper graph) ratios.

Decreasing the hybrid concentration below the K_d value led to a complete inversion of selectivity, in agreement with dissociation of the hybrid. Accordingly, only the complex activity was measured.

The stability of **2**⊂HSA was also studied. Figure 5 shows that after five successive catalytic assays, the selectivity decreased by 10% for an almost constant yield. By comparison, HSA alone lost its specific activity after 650 cycles, and the sulfone product became the major species. Surprisingly, the accumula-

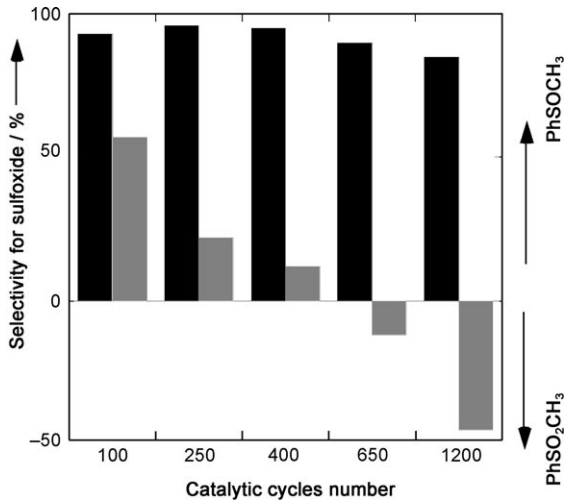

Figure 5. Selectivity for sulfoxide formation versus turnover numbers; **2**⊂HSA (black) and HSA (gray).

tion of sulfoxide resulting from successive oxidation reactions, did not lead to a higher sulfone concentration, as would be the case for the uncatalyzed reaction. This observation suggests that sulfide oxidation catalyzed by the hybrids was much faster than the uncatalyzed oxidation of sulfoxide. This, in turn, precluded any significant use of the oxidant for the latter reaction.

The higher stability of the artificial metalloenzyme was also confirmed by SDS-PAGE (Figure S3). An equal volume of the different catalytic solutions was deposited on a SDS-PAGE gel, and the intensity of the stained protein band was inspected after migration. The bands were more intense for the hybrids than for the native HSA, and no smear was detected in the former case. This suggests that the protein was not degraded in the case of the hybrids.

Surprisingly, the artificial enzyme did not efficiently use hydrogen peroxide as the oxidant. This result contrasts with the good hydrogen peroxide-based activity of Mn–salen complexes bound to engineered apo-myoglobin.[25,26]

The polarizable R groups of the salen ligand affected either the stability or the reactivity of the hybrids, when **2**⊂HSA, **3**⊂HSA and **4**⊂HSA were compared to **1**⊂HSA. Furthermore, the specificity of the catalysis by **2**⊂HSA or **3**⊂HSA, compared to that of the other hybrids, suggests a connection between the selectivity and the nature of the R group.

The stoichiometric addition of thyroxine, ibuprofen or TIB did not alter the catalytic efficiency of the hybrids. This observation confirms that Mn–salen complexes bind tightly to the cleft site of HSA, even under oxidative conditions.

An artificial metalloenzyme is a unique catalyst

The potential uniqueness of artificial enzymes is clearly illustrated by this study. Since sulfone was not produced, the catalytic activity reported herein did not result from the simple combination of the catalytic properties of the two partners of the hybrid. Instead, a genuinely novel reactivity of the complex was generated through its interaction with the protein scaffold. Furthermore, the hybrids catalyzed the sulfoxidation reaction more efficiently than did the complex or HSA alone in terms of both conversion yield and rates.

Although the structural origin of the observed chemoselectivity remains to be established, some reasons for this phenomenon can already be considered. For instance, the protein environment around the complex should be more hydrophobic than that of water. This, in turn, might limit the binding of sulfoxide relative to sulfide, which is significantly less polar. Accordingly, sulfoxide would dissociate before getting further oxidized to sulfone. A similar proposal has been put forward very recently for Mn–salen complexes covalently bound in an engineered myoglobin. However, in that case the selectivity of the protein-free complexes was already high.[42] In our case, a drastic change was observed as the selectivity of the complex alone was inverted for the hybrid. Another possibility is that Mn–salen oxidizing power is tuned through metal coordination by polar amino acid residues. The cleft in HSA contains a majority of Asp and Glu residues, which might be good candidates for binding to the Mn ion. The fact that no oxidation was observed in the presence of hydrogen peroxide suggests that no histidine residue is involved in this dative interaction. Indeed, in the case of hydrogen peroxide-mediated epoxidation, the reactivity of Mn–salen complexes was greatly improved when imidazole was bound in an apical position.[43] Moreover, the absence of intense CD transitions related to the ligand-to-metal charge transfer (LMCT) bands of the inorganic complex in the CD of the hybrid suggests no direct coordination of the Mn. On the other hand, the importance of the R groups for the selectivity of the binding indicates that hydrogen bonding exists between the R groups and residues of the cleft. Asp and Glu residues are good candidates to interact with the R groups.

The increase of yield and stability in the hybrids could also be related to the polarity of the second coordination sphere of the Mn ion. For instance, sulfide molecules could be trapped near the catalyst, increasing the probability for the reaction to occur. Unfortunately, no evidence for sulfide binding has been found using spectroscopic techniques such as CD and UV–visible spectroscopy. It should be noted that even a large sulfide excess did not dissociate the catalyst from the protein.

The substituents of the salen ligand also influence the reactivity of the hybrids as illustrated by **1**⊂HSA being the least selective catalyst. The role of the substituent, at least in the case of carboxylate or sulfonate, was to modulate the binding of the inorganic complex. Thus, the introduction of a carboxylate group reduced the number of binding sites from four in **1**⊂HSA to only one in **2**⊂HSA. These chemical modifications of the salen complex allowed for the design of a stable artificial metalloenzyme and represent a new mode of active site insertion in a protein that does not require amino acid residue coordination. In this case, exclusively supramolecular interactions led to a stable catalyst, even under oxidative conditions.

The only drawback of these hybrids is their inability to provide enantioselectivity (although an interaction between **2** and the protein has been noticed). The apparent inability of the hy-

brids to bind sulfide close to the Mn center might be related to the characteristics of the binding pocket at the protein cleft. This, in turn, might explain the inability of the binding site to discriminate between chiral substrates. The current absence of crystal structures of the hybrids makes the optimization of enantioselectivity a difficult task.

Conclusions

This study demonstrates the potential of artificial metalloenzymes to compete with their natural counterparts in terms of both selectivity and efficiency. The comparison of catalytic efficiency of the complexes and the hybrids shows that the polarity of the protein environment is crucial for selectivity. The next step will be to achieve enantioselective oxidations through genetic manipulations and complex design. Last, but not least, this work illustrates once more the extraordinary ligand-binding repertoire of HSA.

Experimental Section

All chemicals were purchase from Aldrich and used without further purification.

Synthesis of Schiff-base ligands: The salen ligand and the 5,5′-substituted analogues were prepared according to a published procedure.[44] The preparation of the disulfonated salen required the synthesis of the sulfonated salicylaldehyde according to reference [45]

Synthesis of complexes: A mixture of the ligand with $Mn(OAc)_2 \cdot 4H_2O$ (1.5 equiv.) and LiCl (20 equiv.) in $EtOH/H_2O$ was refluxed for 2 h, leading to a green-brown precipitate.

Elemental analysis calcd (%) for complex **1**: $Mn(C_{16}H_{14}N_2O_2)Cl \cdot CH_3CH_2OH \cdot 2H_2O$: C 47.30, H 5.69, N 6,10, Cl 7.76; found: C 47.24, H 4.3, N 6.22, Cl 7.02. ESI-MS for complex **1**: 321 (100%) for $[LMn]^+$ (L corresponds to the dianion of the salen ligand).

Elemental analysis calcd (%) for complex **2**: $Mn(C_{18}H_{13}N_2O_6) \cdot 4H_2O$: C%, 46.89, H 3.9, N 6.07; found: C 46.84, H 4.4, N 6.11. No trace of Cl was found. ESI-MS: 409.2 for $[LMn+H]^+$ (L corresponds to the dianion of the substituted salen).

ESI-MS for complex **3**: 479 for $[LMn-2H^+]^-$ (L corresponds to the dianion of the substituted salen).

Elemental analysis calcd (%) for complex **4**: $Mn(C_{16}H_{14}N_2O_4) \cdot CH_3CH_2OH \cdot 2H_2O$: C 50.04, H 5.4, N 6.45, Mn 12.65; found: C 49.98, H 4.2, N 6.43, Mn 12.10. No trace of Cl was found. ESI-MS: 353 (100%) for $[LMn]^+$ (L corresponds to the dianion of the substituted salen)

Synthesis of hybrids: The synthesis of the hybrids was performed by solubilizing fatty acid-free, globulin-free, lyophilized HSA (Sigma) in Tris buffer (25 mM, pH 8.0, 2.5 mL). The HSA was mixed with a tenfold excess of the Mn complex and incubated overnight at 4 °C. Complexes **3** and **4** were first solubilized in DMSO (5 μL). Excess complex was removed using a desalting column (PD10), leading to the separation of the protein-complex hybrid from the complex solution. The hybrid solution was then dialyzed using a centricon filter with a 30 kDa cut-off (6 cycles) and concentrated to 1.5 mM.

Physical methods: UV–visible absorption spectra were recorded on a Varian Cary1Bio spectrometer, with a quartz cell of 10 mm path length. The concentration of the sample was 100 μM. CD measurements were performed on a JASCO J-810 spectropolarimeter equipped with a thermostated cell holder, using a quartz cell of either 10 mm or 1 mm path length. Spectra were recorded at 25 °C over the 500–250 nm wavelength range at 0.1 nm intervals. Each spectrum was the average of five scans. Tris buffer (50 mM, pH 7.5) was used for all the samples. The use of Tris buffer precluded the recording of data under 250 nm. Fluorescence spectra were recorded on a JASCO FP-6500 spectrofluorometer. All spectra were recorded at 25 °C using a quartz cell of 10 mm path length. Spectra were recorded over the 500–300 nm wavelength range after excitation of the samples at 280 nm. Tris buffer (50 mM, pH 7.5) was used for all the samples.

General protocol for catalysis experiments: Substrate (100 equiv.) and oxidant (200 equiv.) were added to a solution of catalyst (0.04 μmol) in buffer (130 μL, 50 mM) to ensure complete conversion. After the mixture was stirred for 15 min at room temperature, the reference (1 μL, 1 M benzophenone in ethylene chloride) was added. The reaction mixture was then extracted with ethyl acetate (150 μL). An aliquot (1 μL) of the organic phase was injected into the GC without any treatment. Gas chromatography was performed on a Perkin–Elmer Autosystem instrument connected to a PE NELSON 1022 integrator with a FID detector, using a Optima 17 (0.25 μm) column. Injector and detector temperatures were 250 °C, and 280 °C, respectively. The temperature program started at 100 °C for 4 min and then increased at 25 °C min^{-1} over a period of 13 min.

Competitive binding experiments: The hybrid (200 μL, 150 μM) was incubated overnight with an equivalent concentration of drugs corresponding to the number of binding sites in the protein. After one night, the mixture was centrifuged through a Microcon® (Millipore) filter with a 5 KDa cut-off. The filtrate was then analyzed by UV–visible spectroscopy.

Evaluation of hybrid integrity: In order to check the integrity of the hybrid after catalysis we performed SDS-PAGE (with 15% acrylamide).

Acknowledgements

This research was supported by Agence National pour la Recherche (BioInorgCat Project ANR-05-Blan-0042). The authors gratefully acknowledge P. Richaud (CEA, LB3M) for performing the ICP analysis, J.-P Andrieu (IBS) for amino acid analysis, and V. Forge (LCBM) for help with CD experiments.

Keywords: biocatalysis · manganese · metalloenzymes · protein–metal hybrids · sulfide oxidation

[1] H. E. Schoemaker, D. Mink, M. G. Wubbolts, *Science* **2003**, *299*, 1694.
[2] P. T. Anastas, J. B. Zimmerman, *Environ. Sci. Technol.* **2003**, *37*, 95.
[3] Y. Lu, S. M. Berry, T. D. Pfister, *Chem. Rev.* **2001**, *101*, 3047.
[4] Y. Lu, *Inorg. Chem.* **2006**, *45*, 9930.
[5] D. Qi, C.-M. Tann, D. Haring, M. D. Distefano, *Chem. Rev.* **2001**, *101*, 3081.
[6] C. M. Thomas, T. R. Ward, *Chem. Soc. Rev.* **2005**, *34*, 337.
[7] C. Letondor, T. R. Ward, *ChemBioChem* **2006**, *7*, 1845.
[8] U. T. Bornscheuer, R. J. Kazlauskas, *Angew. Chem.* **2004**, *116*, 6156; *Angew. Chem. Int. Ed.* **2004**, *43*, 6032.
[9] Y. Lu, *Curr. Opin. Chem. Biol.* **2005**, *9*, 118.

[10] R. Ricoux, Q. Raffy, J. P. Mahy, *C. R. Chim.* **2007**, *10*, 684.
[11] T. Ueno, S. Abe, N. Yokoi, Y. Watanabe, *Coord. Chem. Rev.* **2007**, *251*, 2717.
[12] E. T. Kaiser, D. S. Lawrence, *Science* **1984**, *226*, 505.
[13] M. E. Wilson, G. M. Whitesides, *J. Am. Chem. Soc.* **1978**, *100*, 306.
[14] M. Skander, N. Humbert, J. Collot, J. Gradinaru, G. Klein, A. Loosli, J. Sauser, A. Zocchi, F. Gilardoni, T. R. Ward, *J. Am. Chem. Soc.* **2004**, *126*, 14411.
[15] T. R. Ward, *Chem. Eur. J.* **2005**, *11*, 3798.
[16] G. Klein, N. Humbert, J. Gradinaru, A. Ivanova, F. Gilardoni, U. E. Rusbandi, T. R. Ward, *Angew. Chem.* **2005**, *117*, 7942; *Angew. Chem. Int. Ed.* **2005**, *44*, 7764.
[17] C. Letondor, N. Humbert, T. R. Ward, *Proc. Natl. Acad. Sci. USA* **2005**, *102*, 4683.
[18] T. Ueno, T. Koshiyama, M. Ohashi, K. Kondo, M. Kono, A. Suzuki, T. Yamane, Y. Watanabe, *J. Am. Chem. Soc.* **2005**, *127*, 6556.
[19] A. Mahammed, H. B. Gray, J. Weaver, K. Sorasenee, Z. Gross, *Bioconjugate Chem.* **2004**, *15*, 738.
[20] R. R. Davies, M. L. Brown, M. Distefano, *Protein Eng.* **1997**, *10*, 61.
[21] T. Kokokubo, T. Sujimoto, T. Uchida, S. Tanimoto, M. Okano, *J. Chem. Soc., Chem. Commun.* **1983**, 769.
[22] a) M. T. Reetz, N. Jiao, *Angew. Chem.* **2006**, *118*, 2476; *Angew. Chem. Int. Ed.* **2006**, *45*, 2416; b) M. Marchetti, G. Mangano, S. Paganelli, C. Botteghi, *Tetrahedron Lett.* **2000**, *41*, 260.
[23] K. Okrasa, R. J. Kazlauskas, *Chem. Eur. J.* **2006**, *12*, 1587.
[24] T. Ueno, N. Yokoi, M. Kono, K. Kondo, A. Suzuki, T. Yamane, Y. Watanabe, *Inorg. Chem.* **2004**, *43*, 2852.
[25] M. Ohashi, T. Koshiyama, T. Ueno, M. Yanase, H. Fujii, Y. Watanabe, *Angew. Chem.* **2003**, *115*, 1035; *Angew. Chem. Int. Ed.* **2003**, *42*, 1005.
[26] J. R. Carey, S. K. Ma, T. D. Pfister, D. K. Garner, H. K. Kim, J. A. Abramite, Z. Wang, Z. Guo, Y. Lu, *J. Am. Chem. Soc.* **2004**, *126*, 10812.
[27] R. Ricoux, E. Lutowska, F. Pezzoti, J. P. Mahy, *Eur. J. Biochem.* **2004**, *271*, 1277.
[28] A. Mahammed, Z. Gross, *J. Am. Chem. Soc.* **2005**, *127*, 2883.
[29] T. Peters, *All About Albumin: Biochemistry, Genetics and Medical Applications*, Academic Press, San Diego, **1995**.
[30] T. Sugimoto, T. Kokubo, J. Miayzaki, S. Tanimoto, M. Okano, *J. Chem. Soc., Chem. Commun.* **1979**, 402.
[31] S. Colonna, S. Banfi, F. Fontana, M. Sommaruga, *J. Org. Chem.* **1985**, *50*, 769.
[32] T. Sugimoto, Y. Matsumara, S. Tanimoto, M. Okano, *J. Chem. Soc., Chem. Commun.* **1978**, 926.
[33] S. Colonna, A. Manfredi, R. Annunziata, *Tetrahedron Lett.* **1988**, *29*, 3343.
[34] J. Larrow, E. N. Jacobsen, *Top. Organomet. Chem.* **2004**, *6*, 123.
[35] K. Srinivasan, P. Michaud, J. K. Kochi, *J. Am. Chem. Soc.* **1986**, *108*, 2309.
[36] M. M. Bradford, *Anal. Biochem.* **1976**, *72*, 248.
[37] C. E. Petersen, C. E. Ha, K. Harohalli, D. Park, N. V. Bhagavan, *Biochemistry* **1997**, *36*, 7012.
[38] U. Kragh-Hansen, *Mol. Pharmacol.* **1988**, *34*, 160.
[39] J. Ghuman, P. A. Zunszain, I. Petitpas, A. A. Bhattacharya, M. Otagiri, S. Curry, *J. Mol. Biol.* **2005**, *353*, 38, and references therein.
[40] F. Nicoletti, B. Howes, M. Fittipaldi, G. Fanali, M. Fasano, P. Ascenzi, G. Smulevich, *J. Am. Chem. Soc.*,DOI: ja8000966t.
[41] O. K. Abou-Zied, O. I. K. Al-Shihi, *J. Am. Chem. Soc.* **2008**, *130*, 10793.
[42] J.-L. Zhang, D. K. Garner, L. Liang, Y. Lu, *Chem. Commun.* **2008**, 1665.
[43] P. Pietikainen, *Tetrahedron* **1998**, *54*, 4319.
[44] P. Pfeiffer, E. Breitha, E. Lubbe, T. Tsumaki, *T. Ann.* **1933**, *503*, 84.
[45] K. J. Berry, F. Moya, K. S. Murray, A. M. B. van den Bergen, B. O. West, *J. Chem. Soc. Dalton Trans.* **1982**, 109.

Received: September 4, 2008
Published online on January 9, 2009

